


Article

The Degradation of Furfural from Petroleum Refinery Wastewater Employing a Packed Bubble Column Reactor Using O₃ and a CuO Nanocatalyst

Safiaa M. Mohammed¹, Ali Abdul Rahman Al Ezzi¹, Hasan Shakir Majdi² and Khalid A. Sukkar^{1,*} 

¹ Department of Chemical Engineering, University of Technology-Iraq, Baghdad 19006, Iraq; che.22.09@grad.uotechnology.edu.iq (S.M.M.); ali.a.nsaif@uotechnology.edu.iq (A.A.R.A.E.)

² Chemical and Petroleum Industries Engineering Department, Al-Mustaqbal University, Babylon 51015, Iraq; dr.hasanshker@mustaqbal-college.edu.iq

* Correspondence: khalid.a.sukkar@uotechnology.edu.iq

Abstract: Furfural is one of the main pollutant materials in petroleum refinery wastewater. This work used an ozonized bubble column reactor to remove furfural from wastewater. The reactor applied two shapes of packing materials and two dosages of CuO nanocatalyst (0.05 and 0.1 ppm) to enhance the degradation process. The results indicated that adding 0.1 ppm of nanocatalyst provided an efficient rate of furfural degradation compared to that of 0.05 ppm. Also, the packing materials enhanced the furfural degradation significantly. As a result, the contact area between the gas and liquid phases increased, and a high furfural removal efficiency was achieved. It was found that the CuO nanocatalyst generated more (OH•) radicals. At a treatment time of 120 min and an ozone flow of 40 L/h, the furfural degradation recorded values of 80.66 and 78.6% at 10 and 20 ppm of initial concentration, respectively. At 60 ppm, the degradation efficiency did not exceed 74.16%. Furthermore, the kinetic study indicated that the first-order mechanism is more favorable than the second-order mechanism, representing the furfural degradation with a correlation factor of 0.9837. Finally, the furfural reaction can be achieved successfully in a shorter time and at low cost.

Keywords: petroleum refinery wastewater; ozonation reaction; furfural degradation; nanocatalyst; advanced oxidation



Citation: Mohammed, S.M.; Al Ezzi, A.A.R.; Majdi, H.S.; Sukkar, K.A. The Degradation of Furfural from Petroleum Refinery Wastewater Employing a Packed Bubble Column Reactor Using O₃ and a CuO Nanocatalyst. *Reactions* **2024**, *5*, 883–899. <https://doi.org/10.3390/reactions5040047>

Received: 30 August 2024

Revised: 26 October 2024

Accepted: 28 October 2024

Published: 11 November 2024



Copyright: © 2024 by the authors. Licensee MDPI, Basel, Switzerland. This article is an open access article distributed under the terms and conditions of the Creative Commons Attribution (CC BY) license (<https://creativecommons.org/licenses/by/4.0/>).

1. Introduction

The production of harmful and toxic chemicals has seen rapid growth with increasing petroleum refinery activities. Large quantities of furfural are used in solvent extraction processes in the petroleum refining industry. Furfural is one of the most toxic and harmful compounds in polluted wastewater produced in many unit operations in petroleum refineries [1–5]. This material has a very dangerous impact on human health and the environment. It has a few exposure routes for entering the human body, including oral, dermal, and nasal. Acute exposure can damage the liver and kidneys; if the exposure continues, it may cause tumors and mutations [2,6]. Different kinds of treatment methods are usually used to remove furfural from wastewater. The general methods include physical, chemical, and biological processes [7–12]. Unfortunately, using these technologies is characterized by some difficulties as well as high energy consumption and high operating costs [13–15]. Usually, the removal of hazardous contaminants such as furfural poses many challenges, which require deep understanding to evaluate reaction mechanisms and process efficiency [8,11,16].

Ozonation technology is one of the most often used advanced oxidation technologies [17–20]. This technology has received increasing attention and is applied to degrade various organic compounds. The main feature of the chemical reaction in this process depends on the oxidation activity of ozone gas. The generation of hydroxyl radicals (OH•)

in the reaction mixture is the chief motivation for the chemical reaction in the process [7,21]. This reaction type is classified as a non-selective chemical oxidation process and has a high efficiency in removing organic compounds from various kinds of wastewater. Usually, the removal of furfural using this technology highly depends on the reactor type. Accordingly, many multiphase reactors have been used such as batch reactors, trickle bed reactors, moving, fluidized bed, and bubble column reactors [22–30]. Among these reactors, the bubble column reactor is considered an important multiphase reactor, which is widely used in chemical industries for carrying out heterogeneous liquid–gas or liquid–gas–solid reactions. This reactor provides high heat and mass transfer rates, handling high operating conditions, and offers efficient mixing and low consumed energy [31–35]. All these factors make the bubble column reactor the efficient reactor, adopted for many treatment processes to remove organic pollutants from industrial wastewater [28,33]. On the other hand, the flow patterns in the bubble column reactor determine the efficiency of the conversion process. The superficial gas velocity is the main parameter in the evaluation of the flow type and the nature of reactor's hydrodynamics parameters [34–39].

Many studies deal with removing furfural and other hydrocarbons from polluted wastewater in the petroleum industry using different reaction technologies. Faramarzpour et al. [40] used TiO_2 Nps as a photocatalyst in the degradation process using a floating-bed photoreactor. They found that 95% removal of furfural can be achieved within two hours. Hosseini et al. [41] used a batch photoreactor to remove furfural using a prepared TiO_2 -clay catalyst. The author noted that UV radiation highly influenced the removal rate of the furfural. Jothinathan et al. [42] applied ozonation technology in the presence of Fe/GAC as a heterogeneous catalyst in a micro-/macro-bubble reactor. The authors observed that the degradation rate achieved was enhanced in the presence of ozone gas. Mousavi and Nezamzadeh [43] studied the degradation of furfural in wastewater using a Fe-clinoptilolite catalyst. They found that the efficiency of the process significantly depends on the operation condition of the reaction. Wei et al. [44] treated phenol using Fe–Mn–Cu/ Al_2O_3 as a heterogeneous catalyst in a rotating packed bed reactor. The authors noted about ~96% of the phenol was removed after 30 min. Rahman [45] used activated carbon in a bubble column reactor to remove phenol from polluted wastewater. The author's results showed that a 90% removal efficiency was achieved. Alattar et al. [46] used ozonation technology to degrade phenol from wastewater using a packed bubble column reactor, finding a conversion efficiency of ~100% at 30 min. Wu et al. [47] studied the activity of prepared CeO_2 in an ozonation reaction to remove three organic pollutants. The authors evaluate the relationship between the degradation rate of organic materials and ozone activity. They found that the reaction mechanism of the degradation process was highly affected by the generated hydroxyl free radical.

The insertion of packing structures into the bubble column reactor will improve the contact surface area between the ozone gas and polluted wastewater. Accordingly, a high rate of organic material conversion will be obtained with high efficiency [15,48]. Usually, a thin film with low resistance to mass transfer will be formed over the packing material. Then, a high degradation rate of organic compounds can be achieved [49–55]. Additionally, the chemical reaction in the ozonation process initiates the formation of hydroxyl radicals which is characterized by their significant influence on the degradation of hydrocarbons into more simple components [24,30,56]. Previous studies have demonstrated that it is still complex to explain how the hydrodynamic behavior affects the process of mass transfer inside the reactor in an ozonation reaction with packing structures. Moreover, the low solubility and high decomposition rate of the ozone gas molecules needs more understanding to evaluate the reaction mechanism [57–61]. These parameters play a constant role in the performance of mass transfer operations between the gas and liquid phases in the reactor. Hence, it is important to recognize the influence of gas velocities on the performance of bubble column reactors [46,62]. Therefore, the main aims of the present investigation are to improve the ozonation process to attain a high level of furfural degradation from the wastewater when using different packing structures in a bubble

column reactor, as well as to evaluate the effect of a heterogeneous nanocatalyst on the reaction efficiency.

2. Materials and Methods

2.1. Chemicals

The experimental work was achieved in a packed bubble column reactor utilizing many chemicals, such as furfural (99.8% purity, Gryfskand Co., Ltd., Fabryczna, Poland); copper oxide nanoparticles were applied as a nanocatalyst in the reactor (97.4% purity) and were purchased from Sigma-Aldrich Company, St. Louis, MO, USA. Additionally, the used packing materials (1.5 cm in diameter and 2.4 g/cm³ of density) were obtained from (QS-Advanced Materials Inc., Troy, MI, USA).

2.2. Experimental Unit

The furfural degradation process was carried out in a packed bubble column reactor (designed and manufactured at Chemical Engineering Department/ University of Technology/ Baghdad-Iraq). Figure 1 represents the schematic diagram of the reaction system and Figure 2 shows the photographs of the experimental apparatus. The reactor dimensions were 1.8 and 0.08 m in height and diameter, respectively. Polluted wastewater with furfural at different concentrations was used as the liquid phase; meanwhile, ozone was used as a gas phase in the ozonation reactor. The ozone gas was supplied from the bottom of the reactor using an OZ/30/Carl-Roth (Karlsruhe, Germany) ozone generation system. Two types of packings were applied to increase the contact area between the gas and liquid phases. The first material was hollow cylinders constructed from glass with a diameter of 20 mm. The second type of packing material was spiral ring structures with a diameter of 3 mm. The reactor was charged with packing up to a level of 120 cm. Additionally, CuO NPs were applied as a heterogeneous catalyst in the ozonation process.

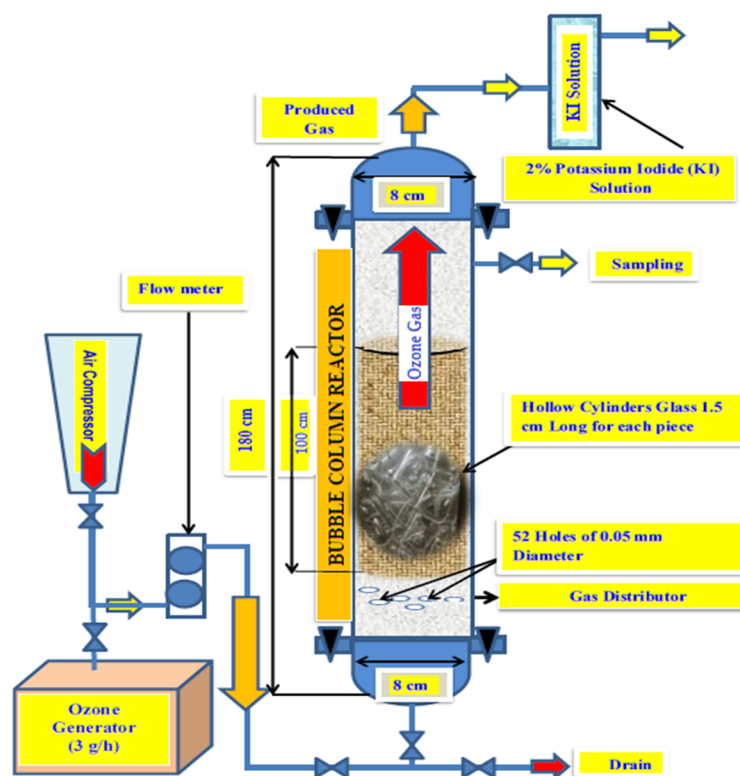


Figure 1. Schematic representation of the ozonized bubble column reactor.



Figure 2. Photograph of the ozonized bubble column reactor apparatus.

The removal of furfural from wastewater was carried out employing two treatment techniques (i.e., ozone gas alone and ozone gas and packing and CuO nanocatalyst). Figure 3 summarizes the two furfural removal techniques. It is important to mention that a stainless-steel gas distributor was fitted at the bottom of the bubble column reactor, including 52 holes, each one being 0.5 mm in size. The flow of ozone gas was controlled using a gas flow meter. Figure 4 shows the ozonized bubble column reactor with uniform small bubbles effecting contact between the gas and liquid phases.

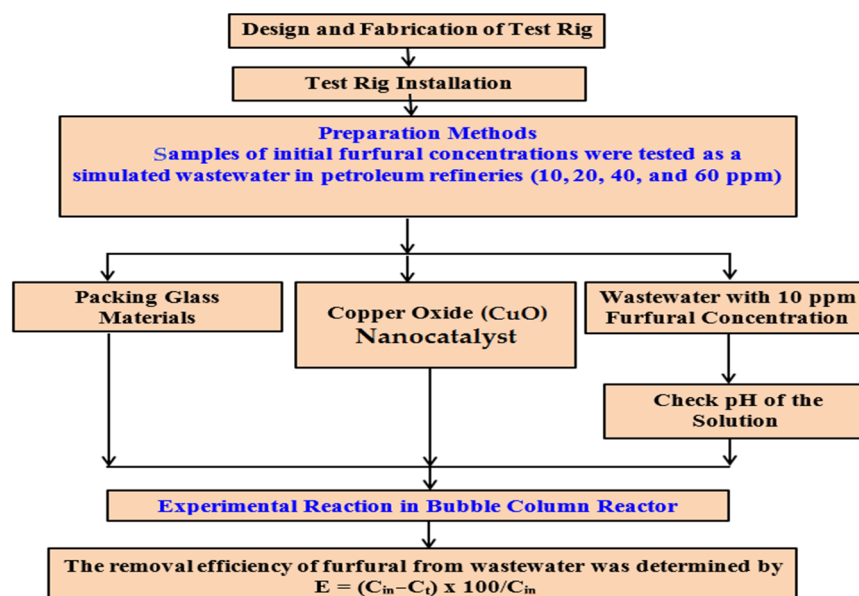


Figure 3. Experimental work summary of furfural removal using ozonized bubble column reactor. Where, E is furfural removal efficient and C_{in} and C_t are the input and residual concentration of furfural.



Figure 4. The contact between the ozone gas and the wastewater mixture in a bubble column reactor using two types of packing materials.

2.3. Furfural Removal Procedure

Four concentrations of furfural were tested (i.e., 10, 20, 40, and 60 ppm), to simulate the range in petroleum industry of polluted wastewater [2,14]. The furfural removal was achieved at different experimental times from 10 to 120 min. A sample of treated mixture at each experimental time was drawn from a valve fitted to the bubble column reactor. On the other hand, the addition of CuO nanocatalyst to the reactor was achieved by mixing the polluted wastewater with a nanocatalyst in a sonication system for 10 min to ensure the formation of a uniform mixture. Two doses of CuO nanocatalyst were used in the reaction process (i.e., 0.05 and 0.1 g/L). In the experimental work, the furfural concentration was achieved based on the determination of the TOC (TOC/L/CSH/E-200 instrument, Shimadzu, Kyoto, Japan). The standard testing method was (ASTM/D7573) [63].

It is important to mention that the ozone generator device supplied ozone gas with an accurate gas-controlling system. This control system was calibrated efficiently according to the procedure of the iodine method cited in the references [12,35]. Then, the concentration of ozone gas was controlled by the flow rate which mainly depended on the supplied pressure from the gas generator.

3. Results and Discussion

3.1. Characterization of CuO Nanocatalyst

Figure 5 shows the XRD pattern results of the CuO nanocatalyst at a 2 theta angle (Shimizu Co., Kyoto, Japan). It was noted that the diffraction peaks of CuO include many characteristic peaks in the structure. These peaks correspond to the specific crystal planes, indicating the formation of monoclinic structure CuO NPs. The used JCPDS number for CuO was (JCPDS 48-1548). Moreover, the appearance of additional diffraction peaks in the nanocatalyst structure indicating the formation of Cu₂O on the material's surface. Accordingly, the well-defined and sharp CuO reflections indicated a good crystalline structure of the CuO nanocatalyst. It is important to mention here that the crystal size of the nanocatalyst is usually related to the highest peaks in the structure. The mean average of the estimated crystal size of the CuO nanocatalyst was 12 nm.

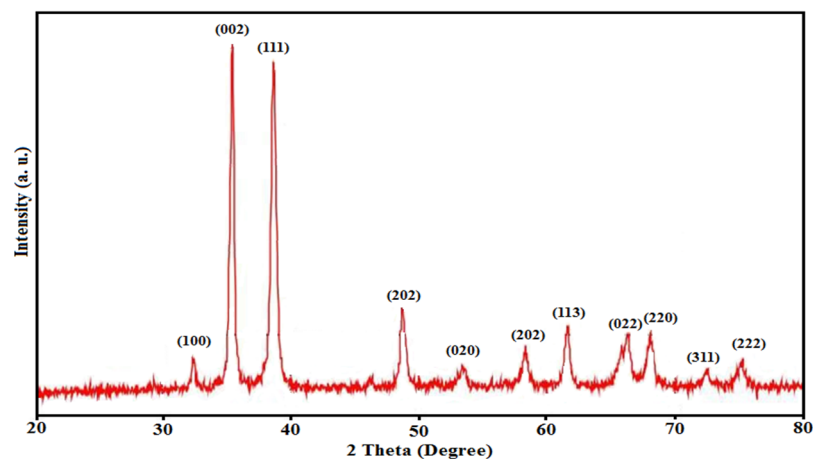


Figure 5. XRD pattern of the CuO nanocatalyst (JCPDS 48-1548).

It is important to mention here that utilizing heterogeneous nanocatalysts in the ozonation reaction is usually applied to improve the degradation of organic materials into CO_2 and H_2O . Therefore, a SEM was used to evaluate the surface morphological characteristics of the CuO nanocatalyst in the reaction system. Figure 6 illustrates the results of the SEM of the CuO nanocatalyst at two magnifications. The SEM results indicate that the morphology of the CuO nanocatalyst has a spherical shape with particle sizes ranging from 20 to 50 nm. This size is appropriate to enhancing the ozonation reaction in the bubble column reactor without any significant variation in the hydrodynamic characteristics of the reactor. A smaller particle size usually provides a larger surface area for the reaction, enhancing the contact between the gas phase and the reaction mixture. Then, it improves the formation of more hydroxyl radicals ($\text{OH}\bullet$) in the reaction mixture. These radicals work as a strong oxidizing agent for furfural in the bubble column reactor.

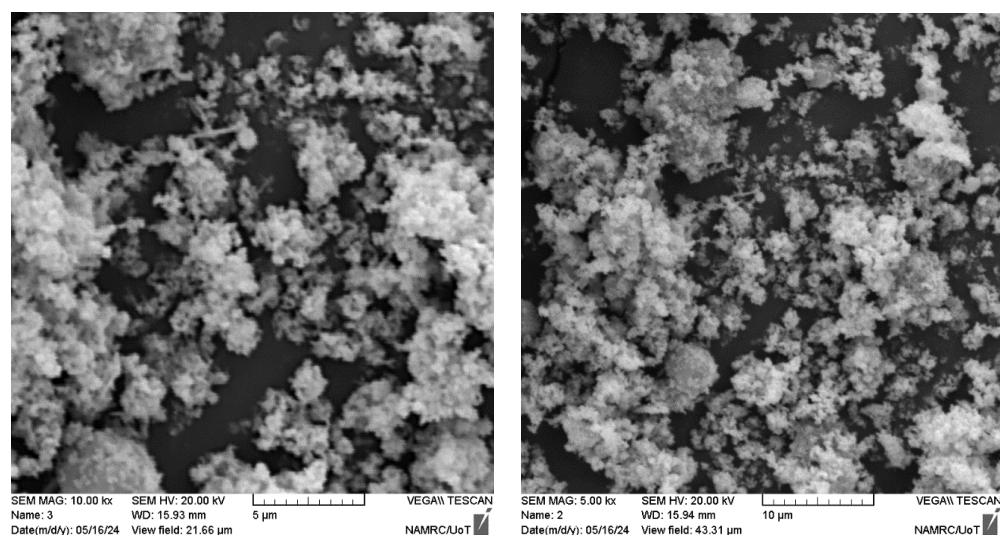


Figure 6. SEM results of the CuO nanocatalyst at two magnifications.

Figure 7 illustrates the FTIR results of the CuO nanocatalyst. Many important functional groups and related bands were noted in the nanocatalyst structure. The general significant bands in the CuO were found at 531 and 603 cm^{-1} , corresponding to the stretching vibration of the Cu–O bond. Strong peaks at 1030 and 1053 cm^{-1} were found in the structure related to C–O stretching vibration. Also, the strong bands at 1604 and 1638 cm^{-1} were due to the aromatic C–C bending vibration. At 2875 and 2884 cm^{-1} , significant bands were also found. These bands are attributed to asymmetric and symmetric C–H

stretching. Furthermore, a band at 1383 cm^{-1} was observed due to the C-N stretching vibration. Finally, O-H stretching was noted for the band at 3439 cm^{-1} .

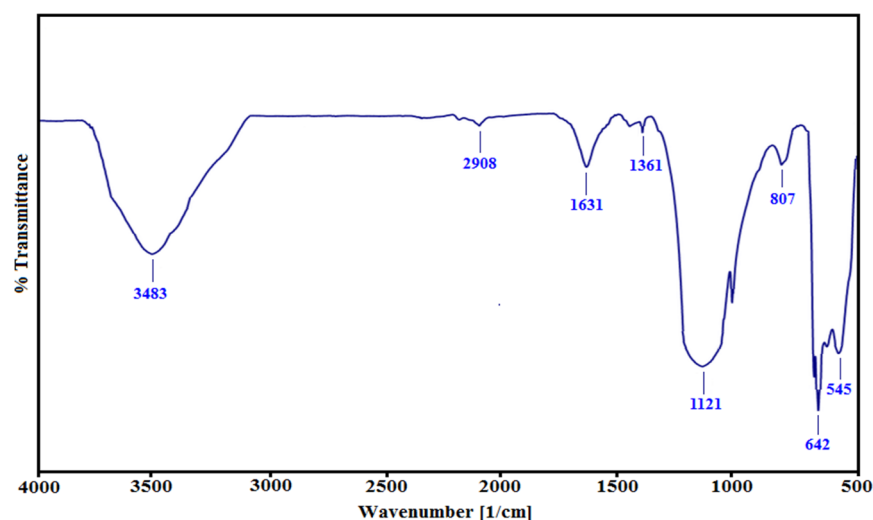


Figure 7. FTIR spectrum of the applied CuO nanocatalyst in the reaction system.

3.2. Furfural Removal in the Presence of Ozone Gas Alone

To evaluate the influence of the concentration of furfural on the removal rate in the bubble column reactor, two concentrations of furfural were tested (i.e., 10 and 20 ppm). The pH of the mixture in the reactor was kept constant at a value of 7. Moreover, the gas phase of the ozone was adjusted to a flow rate of 40 L/h. Figure 8 shows the results of reaction time influencing the removal efficiency at two furfural concentrations in the presence of ozone gas alone in the bubble column reactor. The results of this figure noted that the furfural concentration slightly influences the process of furfural removal with time. At 120 min of reaction time, the highest removal was 72 and 66.9% at 10 and 20 ppm of furfural concentration, respectively. Usually, the chemical reaction was achieved in the reaction mixture due to the activity of hydroxyl radicals ($\text{OH}\bullet$). The degradation process of furfural is highly affected by the reaction mechanism. According to the explanations of many authors, such as [18,32,55], the ozonation reaction in the presence of ozone gas is classified as a low-rate reaction. Therefore, furfural removal efficiency was also limited in this case and required more reaction time.

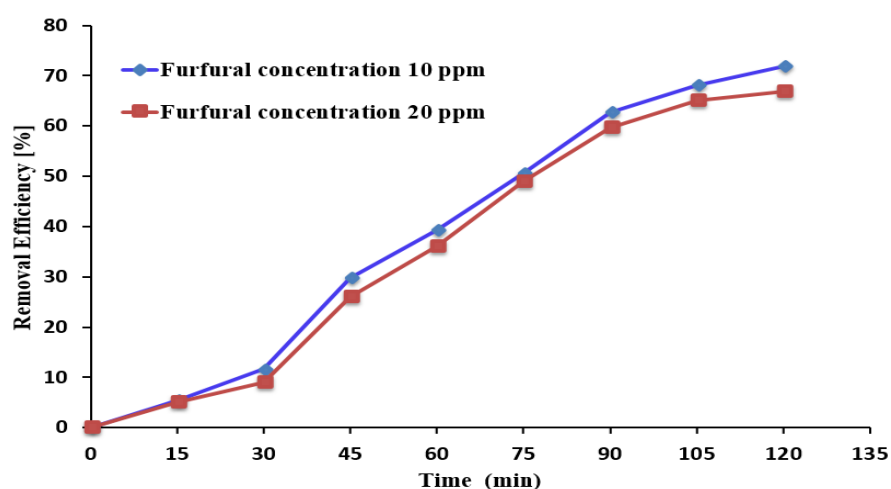


Figure 8. Influence of reaction time on the % removal efficiency at the two furfural concentrations of 10 and 20 ppm (ozone gas alone in the reactor).

3.3. Furfural Removal in the Presence of Ozone and CuO Nanocatalyst

A limited reaction rate usually characterizes the degradation of organic materials in the ozonation reaction. Accordingly, this reaction needs more enhancement by increasing the mass transfer mechanism to form more hydroxyl radicals. According to the notes of many authors, the utilization of nanocatalysts in the ozonation reaction will improve the chemical reaction, and then a high degradation rate will be achieved. In the present work, the CuO nanocatalyst was used for the first time in the ozonation reaction. This material is regarded as a heterogeneous catalyst with a high interfacial surface area. Figure 9a,b summarize the results of the influence of reaction time on furfural removal efficiency in the presence of a CuO nanocatalyst and with glass packing at initial concentrations of 10 and 20 ppm of furfural, respectively. It is important to mention here that the use of glass packing materials in the bubble column reactor was implemented to increase the contact area between the gas and liquid phases in the reaction system.

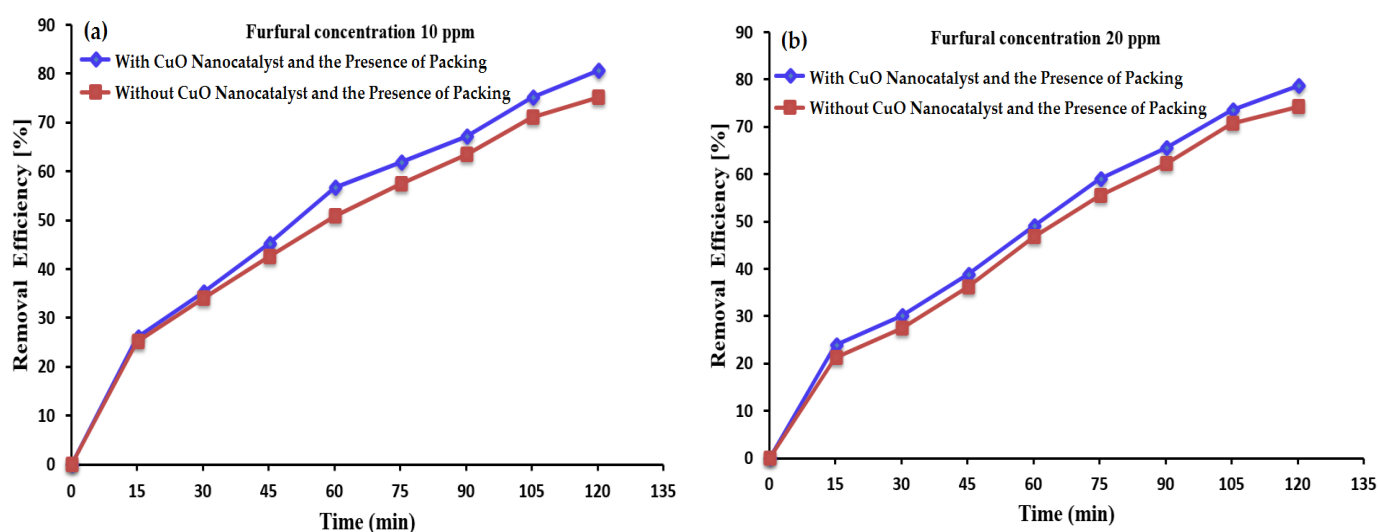


Figure 9. The influence of reaction time on the % removal efficiency in the presence of a CuO nanocatalyst (the dose was 0.1 g/L and the ozone gas flow rate was 40 L/h) and glass packing in a bubble column reactor: (a) in the presence of the CuO nanocatalyst at an initial furfural concentration of 10 ppm and (b) without the CuO nanocatalyst at an initial furfural concentration of 20 ppm.

At an initial furfural concentration of 10 ppm, the results in Figure 9a indicate that the maximum furfural removal efficiency for a reaction time of 120 min and in the absence of the CuO nanocatalyst was 75.2%. On the other hand, the furfural removal efficiency recorded a value of 80.66% in the presence of the CuO nanocatalyst. These results show a clear improvement in the furfural removal efficiency due to the ozonation reaction being enhanced by the influence of the nanocatalyst. This enhancement is attributed to the catalytic activity of the CuO nanocatalyst which enhances the ozonation reaction. Also, the packing material contributes by providing a greater contact area between reaction mixture phases in the reactor. The result show that the highest removal efficiency was achieved at an initial furfural concentration of 10 ppm in comparison with the initial furfural concentration of 20 ppm. At an initial furfural concentration of 20 ppm, the result in Figure 9b shows that the maximum furfural removal efficiencies in the absence or the presence of the CuO nanocatalyst were 74.1 and 78.5%, respectively. Additionally, the furfural degradation reaction was improved due to the generation of more hydroxyl radicals in the reaction mixture resulting from the catalytic activity and packing surface area [5,18,21]. The CuO nanocatalyst initiates the ozonation process, effectively degrading furfural from wastewater at a high reaction rate. This ozonation reaction, in this case, has great potential for treating complex hydrocarbons such as furfurals with high efficiency.

Many authors, such as [11,44,50,52], showed in their results that the presence of nanocatalysts and packing materials in bubble column reactors enhances the removal efficiency of hydrocarbons from wastewater. Four important factors significantly influenced the degradation rate of organic compounds. These are the density of hydroxyl radicals in the reaction mixture, the concentration of organic compounds, the heterogeneous catalyst type, and the available reaction surface area in the reactor. It is important to mention here that the use of an enhanced ozonation process will contribute to a reduction in the consumed energy in the reaction system with high mass transfer, high reaction efficiency, and low economic costs. A significant synergistic influence of both ozone gas and packing material was achieved in the ozonation process for furfural removal. Such behavior provides a high positive contribution to increase furfural degradation efficiency. Moreover, the results in Figure 9 indicate a clear increase in furfural degradation efficiency as a result of using the packing material and nanocatalyst. The same results were noted by [12,30].

3.4. Impact of Initial Furfural Concentrations

Four initial furfural concentrations (i.e., 10, 20, 40, and 60 ppm) were tested in the bubble column reactor using glass packing and a CuO nanocatalyst (0.05 ppm) as shown in Figure 10. This range of concentrations represents the real values of furfural concentrations in wastewater from petroleum refineries [24,30]. From the results of this figure, it can be seen that the furfural degradation efficiency decreases as its initial concentration increases. At a treatment time of 120 min and an ozone flow rate of 40 L/h, the degradation rate of 10 mg/L of furfural reached 80.66%, while it did not exceed 74.16% for 60 mg/L under the same conditions. A dose of 0.05 mg/L of the CuO nanocatalyst provided sufficient hydroxyl radicals to degrade the furfural. Moreover, it was found that the high concentrations of furfural (>40 ppm) need greater reaction times to react and convert to water and carbon dioxide. Generally, the ozonation process with a catalyst and packing material is sufficient to decompose furfural efficiently in a bubble column reactor.

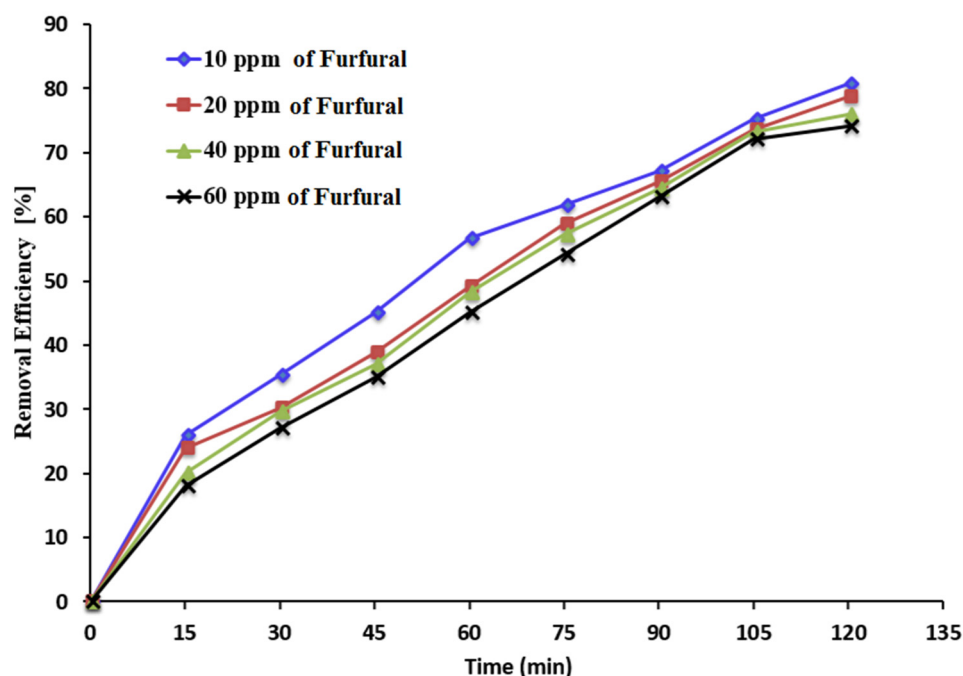


Figure 10. Removal efficiencies of different furfural concentrations using glass packing, CuO nanocatalyst of 0.05 ppm, and ozone flow rate of 40 L/h.

3.5. Influence of the CuO Nanocatalyst Dose on the Removal Efficiency

Figure 11 illustrates the impact of nanocatalyst dose on the removal efficiency of furfural. Two dosages of CuO nanocatalyst were used, 0.05 and 0.1 g/L. In this test, the

furfural concentration was kept constant at 60 ppm. The results in Figure 11 indicate that as the amount of CuO nanocatalyst increased from 0.05 to 0.1 g/L, the removal rate of furfural increased from 74.16 to 79.9%, for an initial furfural concentration of 60 ppm. From a reaction kinetics point of view, the high dosage of nanocatalyst provided more hydroxyl free radicals, and so a higher rate of furfural degradation was achieved. The nanocatalyst also contributed by high contact area between the gas phase and the liquid phase. The same results were noted by [2,15]. Also, it was found that the highest removal efficiency of furfural removal is attributed to the CuO nanocatalyst with a dose of 0.1 g/L, as a result of the availability of CuO nanocatalyst active sites. In this case, a greater furfural degradation rate will be achieved. Additionally, the increased number of active sites initiated the reaction mechanism in the bubble column reactor increasing the reaction rate. Moreover, many authors have indicated that the ozonation reaction is limited due to the nature of the ozone reaction which generates limited hydroxyl free radicals. Accordingly, the addition of CuO nanocatalyst to the reaction mixture increases the furfural degradation rate efficiently by forming more hydroxyl radicals.

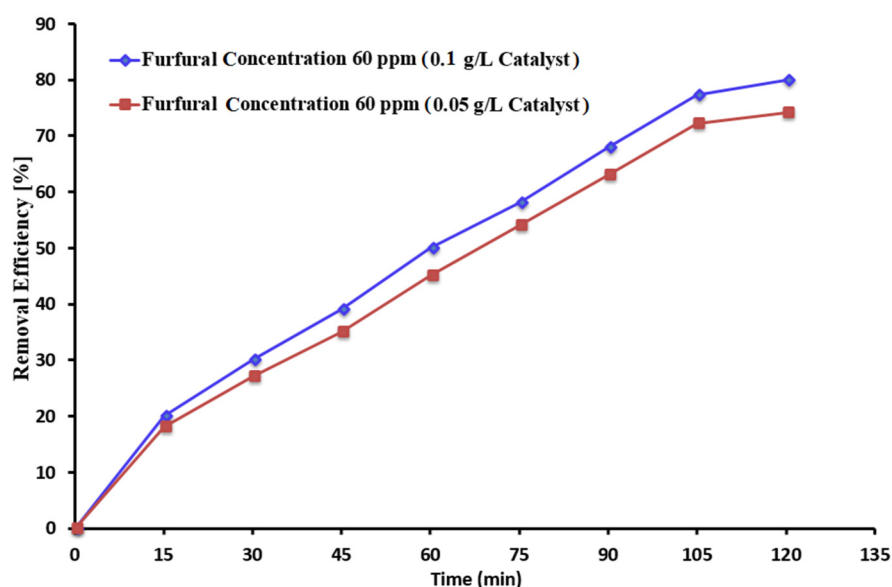


Figure 11. The influence of the nanocatalyst dose on the furfural removal efficiency.

Usually, a high dose of catalyst provides an extended reaction surface area and then more availability of active sites. These factors work on the initiation of the decomposition process of furfural by ozone molecules [12]. Furthermore, the flow rate of ozone and the catalyst activity in the reaction system are the main reasons for the acceleration of the transfer of ozone from the gas phase to the aqueous phase, leading to an increase in the decomposition rate of ozone molecules forming more (OH•) [11]. Furthermore, a packing material usually provides a high interfacial contact area between the gas and liquid phases. This process increases the mass transfer in the reactor, which will contribute to the furfural degradation efficiency in the ozonation reaction. On the other hand, the CuO nanocatalyst works to lower the reaction activation energy and enhance the reaction rate [3,18,45].

3.6. The Impact of the Packing Material

In this section of the experimental work, the contact area between the ozone gas and polluted wastewater in a bubble column reactor was enhanced by utilizing two types of packing materials. The first one is hollow cylinders 2.5 cm high and 1 cm in diameter. The second one is a plastic packing material with multiple fins (see Section 2.2). Figure 12 shows the ozonation reaction in a bubble column reactor in the presence of the two types of packing materials. The chemical reaction was achieved using a CuO nanocatalyst. The results indicated that both glass and plastic packing materials improve the chemical

reaction surface area by providing greater contact between phases. The greater surface area increased the contact time and mass transfer process in the reactor. Such enhancement increases the ability of the reaction to produce hydroxyl routes on the surface of the catalyst. Accordingly, the removal efficiency of the furfural was increased significantly.

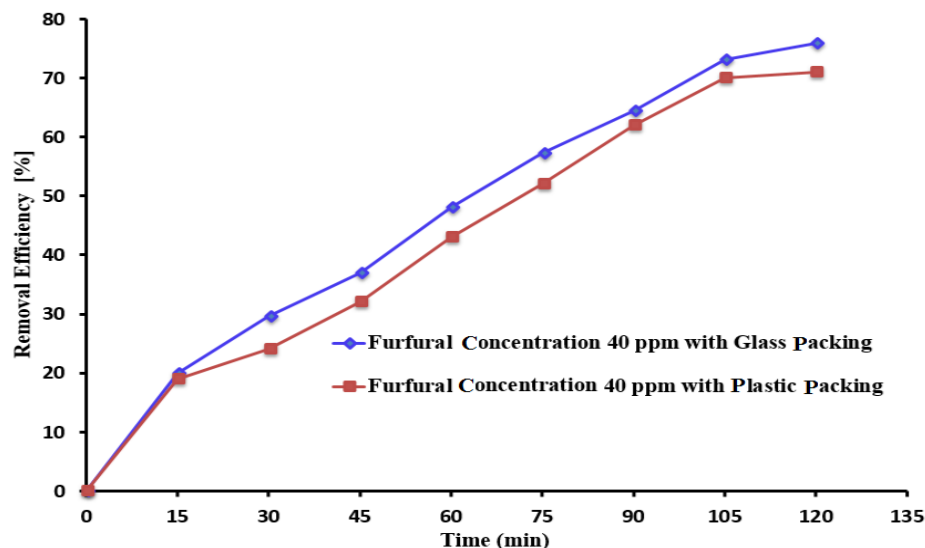


Figure 12. The influence of reaction time on the furfural removal efficiency using different shaped packing materials at an ozone flow rate of 40 L/h.

The highest removal rate of furfural from the chemical reaction was achieved by combining the process in the presence of a packing material. These systems contributed significantly to the increased reaction rate of furfural degradation. Therefore, Figure 12 demonstrates that the furfural removal efficiency increases with increasing contact surface area. Many authors have noted the same results such as Alattar et al. [30], Majhool et al. [35], and Kamarehie et al. [50].

On the other hand, the use of cylindrical packing showed higher rates of furfural removal than the plastic packing material, with an increasing range of 5–8%. This is attributed to the design of the used packing which provides more contact surface area. It is important to mention that during the experimental work, there was no influence of ozone gas on the plastic packing material. The used plastic material is actually a composite material reinforced with ceramic particles so its resistance to any oxidizing agent is high. Accordingly, there was no decline in the ozone concentration in this case. At 120 min of reaction time, the removal percentages of furfural in the presence of glass and plastic packings were 76% and 71%, respectively. These results are consistent with the findings of Li et al. [13], Gao et al. [14], and Wei et al. [15].

3.7. Furfural Degradation Mechanism

For the removal of furfural from wastewater in petroleum refineries, the elimination process requires clear management for many operating parameters. The main parameters are the ozone dose, catalyst type, reaction time, and valuable contact surface area. Accordingly, the ozonation process has been widely applied in the degradation of hydrocarbons. Ozone molecules usually work as a disinfectant and an oxidizing agent in this process. Then, the organic contaminants in wastewater such as furfural will react to simple final compounds such as water and carbon dioxide. Therefore, applying the principles of ozone treatment to wastewater requires a deep understanding of the influence of these factors because the ozone gas reaction usually undergoes a limited reaction rate. The degradation mechanism of furfural enables the reaction paths to operate clearly and safely, which is especially important as furfural presents great danger to human health and the environment [26,33,40].

The analysis of the furfural reaction mechanism in bubble column reactor is highly dependent on the hydrodynamic characteristics of the reactor. It is well known that such reactors are considered complex multiphase reactors. The interaction between the hydrodynamic properties and mass transfer operations are determined by the reaction mechanism and its performance. Accordingly, the utilization of packing material in the bubble column contributes efficiently to increasing the surface area between the ozone and the aqueous phase. This is the main reason why this improves the mass transfer operation and therefore the removal of furfural. From a reaction mechanism point of view, the presence of a packing material in the reactor will contribute to the formation of a thin film of solution mixture over these packing elements (for both types, glass and plastic). This film provides a high mass transfer rate with low resistance and therefore a high furfural degradation efficiency is achieved. Figure 13 summarizes the reaction mechanism of furfural degradation in a bubble column reactor in the presence of a CuO nanocatalyst and packing material. The results of the present investigation show that a significant synergistic impact between the ozone gas phase and the CuO nanocatalyst was achieved. Therefore, furfural degradation by the oxidation and mineralization processes was enhanced dramatically in comparison to the ozonation process alone. Therefore, the combining of ozonation, nanocatalyst, and packing material degrades more furfural within a shorter reaction time.

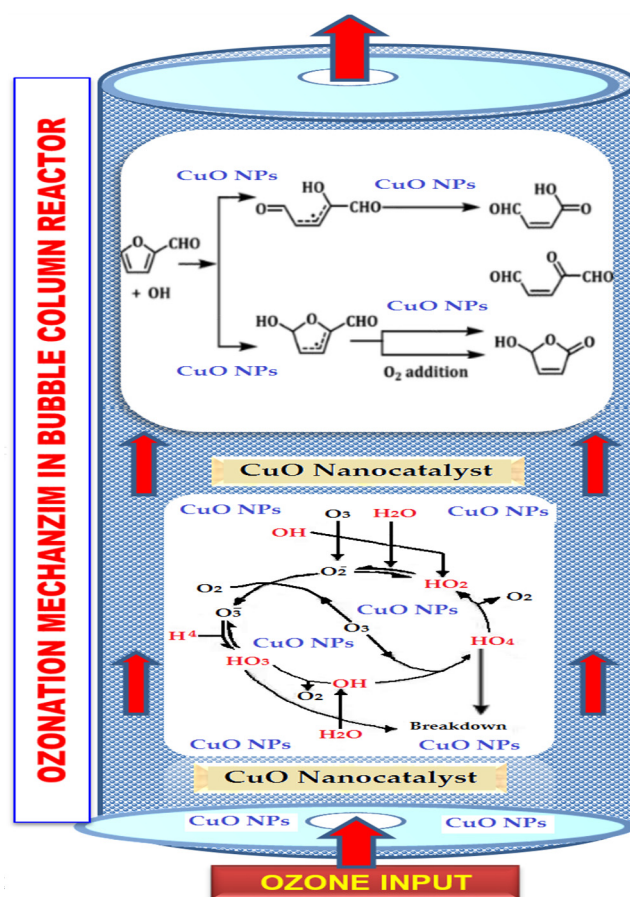


Figure 13. The reaction mechanism of furfural degradation in true bubble column reactor in the presence of the CuO nanocatalyst and the packing material.

Many authors have indicated that ozone gas is an unstable gas and oxidation reactions are usually required to be performed with catalysts to enhance the ozone-supplying process [5,18,21]. Moreover, the mechanisms of ozone adsorption at the surface of heterogeneous catalysts is highly dependent on the ozone molecule and the reaction parameters. It is well known that the ozone gas has weak alkalinity. Therefore, the variation in electron

distribution of the ozone gas molecules looks like a dipole. The central oxygen atom can work as a Lewis acid in the reaction by accepting electrons. On the other hand, the terminal oxygens can work as a Lewis base by providing electrons. Accordingly, the hydroxyl is usually adsorbed at the central or terminal oxygen of the ozone gas and therefore the catalytic ozonation selectivity is enhanced significantly [52,64].

3.8. Kinetics Study of Furfural Degradation

In the present study, the reaction kinetics of furfural degradation with ozone gas were analyzed. The suggested reaction mechanisms depend on the nature of the reaction which is promoted by forming hydroxyl free radicals. Accordingly, two reaction assumptions were suggested (a first-order reaction and a second-order reaction). The reaction rate constants k_1 and k_2 were evaluated according to these assumptions. The estimation process of the reaction rates depended on the furfural concentrations in the mixture inside the reactor and the reaction time (t) [16].

$$\text{For first-order assumption } \ln [R_t/R_0] = -[k_1 t] \quad (1)$$

$$\text{For second-order assumption } R_t = R_0/[1 + R_0 k_2 t] \quad (2)$$

where

R_0 (mg/L) is the initial concentration of furfural at time 0;

R_t (mg/L) is the concentration of the furfural measured at time t;

k_1 (1/min) is the rate constant for the kinetics of the first-order model;

k_2 (L/mg·min) is the rate constant for the kinetics of the second-order model;

t is the reaction time (min).

To evaluate the reaction rate constant of the ozonation process, the best operating conditions for furfural degradation were applied (40 L/h of ozone, 10 ppm of furfural concentration, and 0.05 g/L of CuO nanocatalyst). Also, the experiments were achieved in the presence of a packing material in the reactor.

Figures 14 and 15 show the theoretical and experimental results of the kinetics analysis. The results of the first- and second-order assumption models were achieved depending on Equations (1) and (2), respectively. The determination of the equation slope provides the reaction rate constant (k_1). In the case of the first-order model, the slope was determined by the best fit of $\ln [R_t/R_0]$ vs. the reaction time (t). On the other hand, the reaction rate constant (k_2) of the second-order equation was determined by the slope of the best fit of $[1/R_t]$ vs. the reaction time (t) [17].

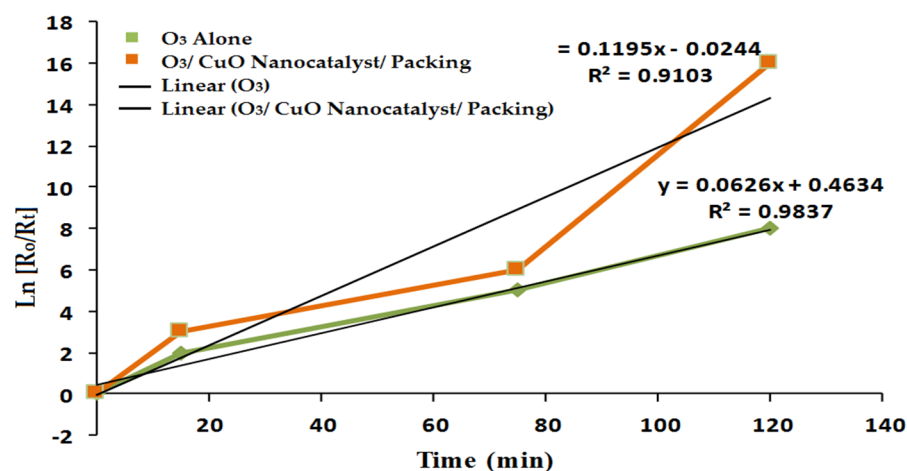


Figure 14. First-order equation of the reaction kinetics of the furfural degradation reaction (The two black lines represent the curve fitting of the O₃ and O₃/CuO Nanocatalyst/ Packings).

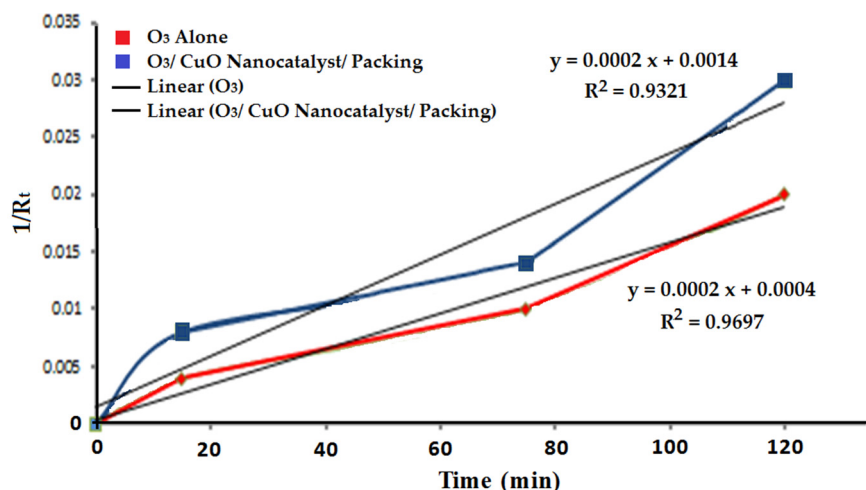


Figure 15. The second-order equation of the reaction kinetics of the furfural degradation reaction (The two black lines represent the curve fitting of the O₃ and O₃/CuO Nanocatalyst/ Packings).

Table 1 summarizes the result of the reaction kinetics assumptions for the first and second orders, respectively. It was found that the kinetics of the reaction between the ozone and the furfural best fit the first-order kinetics. Also, it was found that the highest value of the correction factor in this case was (0.9837). Accordingly, the second-order reaction kinetics assumption for furfural degradation is far from this value. The same results have been found by many authors in ozonation reaction processes such as Dawood and Abdulrazzaq [18] and Barlak et al. [19].

Table 1. The results of kinetics data of the furfural ozonation reaction for the two assumptions.

The First-Order Equation			
Type of treatment	Equation, $Y = \ln(R_0/R_t)$, and $x = t$	k_1 (1/min)	R^2 (L/mg·min)
O ₃ alone	$y = 0.0626x + 0.4634$	0.06712	0.9837
O ₃ /packing/CuO nanocatalyst	$y = 0.1195x - 0.0521$	0.131	0.9103
The Second-Order Equation			
Type of treatment	Equation, $Y = (1/R_t)$, and $x = t$	k_2 (L/mg·min)	R^2 (L/mg·min)
O ₃ alone	$y = 0.0298x + 0.1405$	0.00019	0.9697
O ₃ /packing/CuO nanocatalyst	$y = 0.0002x - 0.0014$	0.00017	0.9321

The results in Figures 14 and 15 indicate that the furfural degradation process in the ozonized packed bubble column in the presence of the CuO nanocatalyst led to a significant increase in the rate constant values. Table 1 presents the results of the k_1 value in the first-order model for each stage of treatment. It is evident that when furfural degradation occurs using ozone alone, and using O₃-packing-CuO nanocatalyst, the k_1 values were 0.067 and 0.131, respectively. These findings highlight the substantial impact of utilizing packing in a bubble column reactor in combination with a CuO nanocatalyst to achieve a higher value of the reaction rate constant (k_1) with a high value of the relation coefficient (R^2) in the first-order model in the ozonation reaction.

4. Conclusions

The low solubility of ozone in reaction mixtures lowers the utility of ozone gas in reaction systems. Then, the furfural degradation efficiency in wastewater was enhanced by using glass packing materials and a CuO nanocatalyst. The results indicate that the best CuO nanocatalyst weight for treating wastewater was 0.1 g/L. Additionally, the experimental results showed that the O₃-glass-CuO nanocatalyst reaction system resulted

in a greater furfural removal rate (86%) for a reaction time of 60 min and an initial furfural dose of 15 ppm. It was found that the CuO nanocatalyst enhanced the catalytic ozonation reaction due to the high number of active sites within the catalyst structure. Furthermore, the presence of a packing material in the reactor improves the ozonation process due to the greater contact area between the gas and liquid phases it provides. It is important to mention that there are no previous investigations that have used the furfural ozonation reaction combined with CuO nanocatalysts in the presence of a packing material in a bubble column reactor. Additionally, this study shows greater understanding of the ozonation reaction used to remove furfural from polluted wastewater within a shorter contact time. The kinetic study indicated that the first-order mechanism is more favorable in terms of representing the furfural degradation process in comparison to that of the second-order by a correlation factor of 0.9837.

Author Contributions: Conceptualization, K.A.S. and A.A.R.A.E.; methodology, S.M.M.; formal analysis, S.M.M.; investigation, K.A.S. and A.A.R.A.E.; data curation, S.M.M. and A.A.R.A.E.; writing—original draft preparation, S.M.M.; writing—review and editing, K.A.S.; visualization, A.A.R.A.E.; supervision, K.A.S. and H.S.M.; project administration, K.A.S. and H.S.M. All authors have read and agreed to the published version of the manuscript.

Funding: This research received no external funding.

Data Availability Statement: The original contributions presented in this study are included in the article. Further inquiries can be directed to the corresponding author.

Acknowledgments: The authors are grateful to the Chemical Engineering, University of Technology, Iraq, and Al-Mustaqbal University, Babylon, Iraq, for their scientific support of this study.

Conflicts of Interest: The authors declare no conflicts of interest.

References

1. Zhang, J.; Shao, S.; Ding, X.; Li, Z.; Jing, J.; Jiao, W.; Liu, Y. Removal of phenol from wastewater by high-gravity intensified heterogeneous catalytic ozonation with activated carbon. *Environ. Pollut.* **2022**, *29*, 34830–34840. [[CrossRef](#)] [[PubMed](#)]
2. Dalali, N.; Kazeraninejad, M.; Akhavan, A. Treatment of petroleum refinery wastewater containing furfural by electron beam irradiation. *Desalination Water Treat.* **2016**, *57*, 24124–24131. [[CrossRef](#)]
3. Guo, H.; Qin, Q.; Hu, M.; Chang, J.S.; Lee, D.J. Treatment of refinery wastewater: Current status and prospects. *J. Environ. Chem. Eng.* **2024**, *12*, 112508. [[CrossRef](#)]
4. Pourali, P.; Fazlzadeh, M.; Aaligadri, M.; Dargahi, A.; Poureshgh, Y.; Kakavandi, B. Enhanced three-dimensional electrochemical process using magnetic recoverable of Fe₃O₄@GAC towards furfural degradation and mineralization. *Arab. J. Chem.* **2022**, *15*, 103980. [[CrossRef](#)]
5. Ghosh, S.; Falyouna, O.; Malloum, A.; Othmani, A.; Bornman, C.; Bedair, H.; Onyeaka, H.; Al-Sharify, Z.T.; Jacob, A.O.; Miri, T.; et al. A general review on the use of advance oxidation and adsorption processes for the removal of furfural from industrial effluents. *Microporous Mesoporous Mater.* **2022**, *331*, 111638. [[CrossRef](#)]
6. Majhool, A.; Sukkar, K.; Alsaffar, M. Combining α -Al₂O₃ packing material and a ZnO nanocatalyst in an ozonized bubble column reactor to increase the phenol degradation from wastewater. *Processes* **2023**, *11*, 2416. [[CrossRef](#)]
7. Contreras-Zarazúa, G.; Jasso-Villegas, M.E.; Ramírez-Márquez, C.; Sánchez-Ramírez, E.; Vázquez-Castillo, J.A.; Segovia-Hernandez, J.G. Design and intensification of distillation processes for furfural and co-products purification considering economic, environmental, safety and control issues. *Chem. Eng. Process.-Process Intensif.* **2021**, *159*, 108218. [[CrossRef](#)]
8. Barlak, M.S.; Değermenci, N.; Cengiz, I.; Özel, H.U.; Yildiz, E. Comparison of phenol removal with ozonation in jet loop reactor and bubble column. *J. Environ. Chem. Eng.* **2020**, *8*, 104402. [[CrossRef](#)]
9. Jin, X.; Wu, C.; Fu, L.; Tian, X.; Wang, P.; Zhou, Y.; Zuo, J. Development, dilemma and potential strategies for the application of nanocatalysts in wastewater catalytic ozonation: A review. *J. Environ. Sci.* **2023**, *124*, 330–349. [[CrossRef](#)]
10. Grmasha, R.A.; Stenger-Kovács, C.; Bedewy, B.A.H.; Al-Sareji, O.J.; Al-Juboori, R.A.; Meiczinger, M.; Hashim, K.S. Ecological and human health risk assessment of polycyclic aromatic hydrocarbons (PAH) in Tigris river near the oil refineries in Iraq. *Environ. Res.* **2023**, *227*, 115791. [[CrossRef](#)]
11. Kermani, M.; Farzadkia, M.; Morovati, M.; Taghavi, M.; Fallahizadeh, S.; Khaksefidi, R.; Norzaee, S. Degradation of furfural in aqueous solution using activated persulfate and peroxymonosulfate by ultrasound irradiation. *J. Environ. Manag.* **2020**, *266*, 110616. [[CrossRef](#)] [[PubMed](#)]
12. Alattar, S.; Sukkar, K.; Alsaffar, M. The role of TiO₂ NPs catalyst and packing material in removal of phenol from wastewater using an ozonized bubble column reactor. *Acta Innov.* **2023**, *46*, 90–101. [[CrossRef](#)]

13. Shabanloo, A.; Salari, M.; Shabanloo, N.; Dehghani, M.H.; Pittman, C.U., Jr.; Mohan, D. Heterogeneous persulfate activation by nano-sized Mn_3O_4 to degrade furfural from wastewater. *J. Mol. Liq.* **2020**, *298*, 112088. [[CrossRef](#)]
14. Nsaif-Al Ezzi, A.A.R.; Balasim, N. Removal of chloroform and phenol from water by expanded bed air lift loop reactor. *Solid State Technol.* **2020**, *63*, 5213–5223.
15. Khudhair, H.A.; Ismail, Z.Z. New application of single and mixed immobilized cells for furfural biodegradation. *Bioremediat. J.* **2019**, *23*, 32–41. [[CrossRef](#)]
16. Cheng, P.; Huang, J.; Song, X.; Yao, T.; Jiang, J.; Zhou, C.; Yan, X.; Ruan, R. Heterotrophic and mixotrophic cultivation of microalgae to simultaneously achieve furfural wastewater treatment and lipid production. *Bioresour. Technol.* **2022**, *349*, 126888. [[CrossRef](#)]
17. Alomar, T.; Hameed, B.H.; Al-Ghouti, M.A.; Almomani, F.A.; Han, D.S. A review on recent developments and future prospects in the treatment of oily petroleum refinery wastewater by adsorption. *J. Water Process Eng.* **2024**, *64*, 105616. [[CrossRef](#)]
18. Shokoohi, R.; Bajalan, S.; Salari, M.; Shabanloo, A. Thermochemical degradation of furfural by sulfate radicals in aqueous solution: Optimization and synergistic effect studies. *Environ. Sci. Pollut. Res.* **2019**, *26*, 8914–8927. [[CrossRef](#)]
19. Zhou, L.; Zhang, S.; Li, Z.; Liang, X.; Zhang, Z.; Liu, R.; Yun, J. Efficient degradation of phenol in aqueous solution by catalytic ozonation over MgO/AC . *J. Water Process Eng.* **2020**, *36*, 101168. [[CrossRef](#)]
20. Derco, J.; Gotvajn, A.Ž.; Čizmarová, O.; Dudáš, J.; Sumegová, L.; Šimovičová, K. Removal of micropollutants by ozone-based processes. *Processes* **2021**, *9*, 1013. [[CrossRef](#)]
21. Mohamadi, L.; Bazrafshan, E.; Rahdar, A.; Labuto, G.; Kamali, A.R. Nanostructured MgO -enhanced catalytic ozonation of petrochemical wastewater. *Boletín Soc. Española Cerámica Vidr.* **2021**, *60*, 391–400. [[CrossRef](#)]
22. Zhang, F.; Wei, C.; Hu, Y.; Wu, H. Zinc ferrite catalysts for ozonation of aqueous organic contaminants: Phenol and bio-treated coking wastewater. *Sep. Purif. Technol.* **2015**, *156*, 625–635. [[CrossRef](#)]
23. Li, X.; Fu, L.; Chen, F.; Zhao, S.; Zhu, J.; Yin, C. Application of heterogeneous catalytic ozonation in wastewater treatment: An overview. *Catalysts* **2023**, *13*, 342. [[CrossRef](#)]
24. Cao, Q.; Sang, L.; Tu, J.; Xiao, Y.; Liu, N.; Wu, L.; Zhang, J. Rapid degradation of refractory organic pollutants by continuous ozonation in a micro-packed bed reactor. *Chemosphere* **2021**, *270*, 128621. [[CrossRef](#)]
25. Dehdar, A.; Rahmani, A.R.; Azarian, G.; Jamshidi, R.; Moradi, S. Removal of furfural using zero gap electrocoagulation by a scrap iron anode from aqueous solution. *J. Mol. Liq.* **2022**, *367*, 120368. [[CrossRef](#)]
26. Zabermaawi, N.M.; Bestawy, E.E. Effective treatment of petroleum oil-contaminated wastewater using activated sludge modified with magnetite/silicon nanocomposite. *Environ. Sci. Pollut. Res.* **2024**, *31*, 17634–17650. [[CrossRef](#)]
27. Ezzi, R.A.; Abdul, A.; Alhamdiny, S.H. A new treatment design for water contaminated with phenol. *Environ. Health Eng. Manag. J.* **2019**, *6*, 185–190. [[CrossRef](#)]
28. Mousa, N.E.; Mohammed, S.S.; Shnain, Z.Y.; Abid, M.F.; Alwasiti, A.A.; Sukkar, K.A. Catalytic photodegradation of cyclic sulfur compounds in a model fuel using a bench-scale falling-film reactor irradiated by a visible light. *Bull. Chem. React. Eng. Catal.* **2022**, *17*, 755–767. [[CrossRef](#)]
29. Can-Güven, E.; Daniser, Y.; Guvenc, S.Y.; Ghanbari, F.; Varank, G. Effective removal of furfural by ultraviolet activated persulfate, peroxide, and percarbonate oxidation: Focus on influencing factors, kinetics, and water matrix effect. *J. Photochem. Photobiol. A Chem.* **2022**, *433*, 114139. [[CrossRef](#)]
30. Alattar, S.A.; Sukkar, K.A.; Alsaffar, M.A. Phenol removal from wastewater in petroleum refineries by managing flow characteristics and nanocatalyst in ozonized bubble column. *Pet. Chem.* **2024**, *64*, 159–169. [[CrossRef](#)]
31. Chen, C.; Yoza, B.A.; Wang, Y.; Wang, P.; Li, Q.X.; Guo, S.; Yan, G. Catalytic ozonation of petroleum refinery wastewater utilizing $Mn-Fe-Cu/Al_2O_3$ catalyst. *Environ. Sci. Pollut. Res.* **2015**, *22*, 5552–5562. [[CrossRef](#)]
32. Hamied, R.S.; Sukkar, K.A.; Majdi, H.S.; Shnain, Z.Y.; Graish, M.S.; Mahmood, L.H. Catalytic-level identification of prepared Pt/HY , $Pt-Zn/HY$, and $Pt-Rh/HY$ nanocatalysts on the reforming reactions of n-Heptane. *Processes* **2023**, *11*, 270. [[CrossRef](#)]
33. Wang, B.; Zhang, H.; Wang, F.; Xiong, X.; Tian, K.; Sun, Y.; Yu, T. Application of heterogeneous catalytic ozonation for refractory organics in wastewater. *Catalysts* **2019**, *9*, 241. [[CrossRef](#)]
34. Zoumpouli, G.A.; Zhang, Z.; Wenk, J.; Prasse, C. Aqueous ozonation of furans: Kinetics and transformation mechanisms leading to the formation of α , β -unsaturated dicarbonyl compounds. *Water Res.* **2021**, *203*, 117487. [[CrossRef](#)]
35. Majhool, A.K.; Sukkar, K.A.; Alsaffar, M.A.; Majdi, H.S. Integrated process for high phenol removal from wastewater employing a ZnO nanocatalyst in an ozonation reaction in a packed bubble column reactor. *ChemEngineering* **2023**, *7*, 112. [[CrossRef](#)]
36. Wang, S.; Ma, J.; Li, H.; Li, G.; Zhou, L.; Cao, X.; Yun, J. Mineralization of high concentration of aniline and other organics in wastewater by catalytic ozonation on $CaMn_2O_4$. *J. Water Process Eng.* **2024**, *60*, 105160. [[CrossRef](#)]
37. Wang, C.; Zhou, G.; Xu, Y.; Yu, P. The Effect of Magnetic Composites ($\gamma-Al_2O_3/TiO_2/\gamma-Fe_2O_3$) as Ozone Catalysts in Wastewater Treatment. *Materials* **2022**, *15*, 8459. [[CrossRef](#)]
38. Zhang, S.; Wang, D.; Fan, P.P.; Zhou, L. Zeolite-induced catalytic ozonation of p-aminobenzenesulfonic acid in a bubbling reactor. *Desalination Water Treat.* **2016**, *57*, 1949–1958. [[CrossRef](#)]
39. Al Ezzi, A.A.R. Removal of phenol by expanded bed airlift loop reactor. *Iran. J. Chem. Chem. Eng.* **2022**, *41*, 154–162.
40. Faramarzpour, M.; Vossoughi, M.; Borghei, M. Photocatalytic degradation of furfural by titania nanoparticles in a floating-bed photoreactor. *Chem. Eng. J.* **2009**, *146*, 79–85. [[CrossRef](#)]
41. Hosseini, L.; Ghafurian, N.; Hosseini, S.N.; Hassanzadeh, S.M. Immobilization of TiO_2 on leca granules for photocatalytic degradation of furfural. *Casp. J. Appl. Sci. Res.* **2014**, *3*, 23.

42. Jothinathan, L.; Cai, Q.Q.; Ong, S.L.; Hu, J.Y. Organics removal in high strength petrochemical wastewater with combined microbubble-catalytic ozonation process. *Chemosphere* **2021**, *263*, 127980. [[CrossRef](#)]
43. Mousavi-Mortazavi, S.; Nezamzadeh-Ejhih, A. Supported iron oxide onto an Iranian clinoptilolite as a heterogeneous catalyst for photodegradation of furfural in a wastewater sample. *Desalination Water Treat.* **2016**, *57*, 10802–10814. [[CrossRef](#)]
44. Wei, X.; Shao, S.; Ding, X.; Jiao, W.; Liu, Y. Degradation of phenol with heterogeneous catalytic ozonation enhanced by high gravity technology. *J. Clean. Prod.* **2020**, *248*, 119179. [[CrossRef](#)]
45. Rahman, A.A. Phenol removal using pulsation bubble column with inverse fluidization airlift loop reactor. *Chem. Ind. Chem. Eng. Q.* **2021**, *27*, 99–106.
46. Alattar, S.A.; Sukkar, K.A.; Alsaffar, M.A. Enhancement of ozonation reaction for efficient removal of phenol from wastewater using a packed bubble column reactor. *Indones. J. Chem.* **2023**, *23*, 383–394. [[CrossRef](#)]
47. Bello, M.M.; Y'ng, T.S.; Abdul Raman, A.A. Response surface methodology optimization of integrated fluidized bed adsorption–Fenton oxidation for removal of Reactive Black 5. *Chem. Eng. Commun.* **2020**, *207*, 1567–1578. [[CrossRef](#)]
48. Abid, M.F.; Alwan, G.M.; Abdul-Ridha, L.A. Study on catalytic wet air oxidation process for phenol degradation in synthetic wastewater using trickle bed reactor. *Arab. J. Sci. Eng.* **2016**, *41*, 2659–2670. [[CrossRef](#)]
49. Das, A.; Adak, M.K.; Mahata, N.; Biswas, B. Wastewater treatment with the advent of TiO₂ endowed photocatalysts and their reaction kinetics with scavenger effect. *J. Mol. Liq.* **2021**, *338*, 116479. [[CrossRef](#)]
50. Kamarehie, B.; Jafari, A.; Ghaderpoori, M.; Amin Karami, M.; Mousavi, K.; Ghaderpoury, A. Catalytic ozonation process using PAC/γ-Fe₂O₃ to Alizarin Red S degradation from aqueous solutions: A batch study. *Chem. Eng. Commun.* **2019**, *206*, 898–908. [[CrossRef](#)]
51. Chen, J.; Tian, S.; Kong, L.; Tu, Y.; Lu, J.; Xiong, Y. Efficient degradation of nitrobenzene by an integrated heterogeneous catalytic ozonation and membrane separation system with active MgO (111) catalyst. *Desalination Water Treat.* **2015**, *56*, 2168–2180. [[CrossRef](#)]
52. Duan, L.; Ma, C.; Lou, F.; Yin, J.; Sang, L.; Zhang, J. Investigation of external mass transfer in a micropacked bed reactor with a Pd/Al₂O₃/nickel foam. *Ind. Eng. Chem. Res.* **2022**, *61*, 13710–13719. [[CrossRef](#)]
53. Gholami, N.; Ghasemi, B.; Anvaripour, B.; Jorfi, S. Enhanced photocatalytic degradation of furfural and a real wastewater using UVC/TiO₂ nanoparticles immobilized on white concrete in a fixed-bed reactor. *J. Ind. Eng. Chem.* **2018**, *62*, 291–301. [[CrossRef](#)]
54. Veisi, F.; Zazouli, M.A.; Ebrahimzadeh, M.A.; Charati, J.Y.; Dezfoli, A.S. Photocatalytic degradation of furfural in aqueous solution by N-doped titanium dioxide nanoparticles. *Environ. Sci. Pollut. Res.* **2016**, *23*, 21846–21860. [[CrossRef](#)]
55. Mazumder, A.; Sarkar, S.; Sen, D.; Bhattacharjee, C. Environmental effects and human health challenges originated from oily wastewater. In *Advanced Technologies in Wastewater Treatment*; Elsevier: Amsterdam, The Netherlands, 2023; pp. 29–47.
56. Gu, Y.; Dai, P.; Wu, T.; Yuan, F.; Yang, Q. A novel physical-biochemical treatment of refinery wastewater. *J. Environ. Manag.* **2024**, *354*, 120356. [[CrossRef](#)]
57. Ismail, Z.Z.; Jasim, A.S. Ultrasonic treatment of wastewater contaminated with furfural. *IDA J. Desalination Water Reuse* **2014**, *6*, 103–111. [[CrossRef](#)]
58. Ayhan, N.N.; Aldemir, A.; Özgüven, A. Treatment of petroleum refinery wastewater by chemical coagulation method: Determination of optimum removal conditions using experimental design. *Braz. J. Chem. Eng.* **2024**, *41*, 121–137. [[CrossRef](#)]
59. Mohammed, A.A.; Sukkar, K.A.; Shnain, Z.Y. Effect of graphene and multiwalled carbon nanotube additives on the properties of nano-reinforced rubber. *Chem. Pap.* **2021**, *75*, 3265–3272. [[CrossRef](#)]
60. Baqur, M.S.; Hamied, R.S.; Sukkar, K.A. An eco-friendly process to produce high-purity nano-γ-Al₂O₃ from aluminum scrap using a novel electrolysis technique for petroleum industry applications. *Arab. J. Sci. Eng.* **2023**, *48*, 15915–15925. [[CrossRef](#)]
61. Wang, J.; Smit, M.G.; Verhaegen, Y.; Nolte, T.M.; Redman, A.D.; Hendriks, A.J.; Hjort, M. Petroleum refinery effluent contribution to chemical mixture toxic pressure in the environment. *Chemosphere* **2023**, *311*, 137127. [[CrossRef](#)]
62. Al-Tameemi, H.M.; Sukkar, K.A.; Abbar, A.H. Treatment of petroleum refinery wastewater by a combination of anodic oxidation with photocatalyst process: Recent advances, affecting factors and future perspectives. *Chem. Eng. Res. Des.* **2024**, *204*, 487–508. [[CrossRef](#)]
63. ASTM D7573; Standard Test Method for Total Carbon and Organic Carbon in Water by High Temperature Catalytic Combustion and Infrared Detection. ASTM: West Conshohocken, PA, USA, 2017.
64. Luo, X.; Su, T.; Xie, X.; Qin, Z.; Ji, H. The adsorption of ozone on the solid catalyst surface and the catalytic reaction mechanism for organic components. *ChemistrySelect* **2020**, *5*, 15092–15116. [[CrossRef](#)]

Disclaimer/Publisher's Note: The statements, opinions and data contained in all publications are solely those of the individual author(s) and contributor(s) and not of MDPI and/or the editor(s). MDPI and/or the editor(s) disclaim responsibility for any injury to people or property resulting from any ideas, methods, instructions or products referred to in the content.